

Novel Liquid Crystalline Organic–Inorganic Hybrid for Highly Sensitive Photoinscriptions

Kaori Nishizawa,^{†,‡} Shusaku Nagano,[†] and Takahiro Seki*[†]

[†]Department of Molecular Design and Engineering, Graduate School of Engineering, Nagoya University, Chikusa, Nagoya 464-8603, Japan, and [‡]National Institute of Advanced Industrial Science and Technology (AIST), Moriyama, Nagoya 463-8560, Japan

Received December 2, 2008. Revised Manuscript Received May 1, 2009

A new class of organic–inorganic liquid crystalline hybrid materials consisting of an azobenzene derivative and titanium oxide (6Az5COO-TiO and 6Az1COO-TiO) was synthesized. 6Az5COO-TiO with a C5 spacer showed a smectic liquid crystalline phase. The organic 6Az5COO and TiO inorganic components in the hybrid film were oriented perpendicular and parallel to the substrate plane, respectively, to form a layered structure. The structure of the liquid crystalline hybrid material was formed via nanophase separation of the organic and inorganic components. This film was then subjected to the inscription of surface relief structure formation by patterned UV irradiation. The efficiency of the phototriggered mass transfer showed a clear temperature dependency. The optimal temperature range was around 130 °C, which corresponds to the lower edge of the endothermic peak in the differential scanning calorimetric profile. The mass transfer was initiated at a surprisingly small energy dose of irradiation [40 mJ cm⁻² (8 mW cm⁻² for 5 s)] in this hybrid material, as has been observed for fully organic soft liquid crystalline polymer systems. It is anticipated that this new type of hybrid material have potential for microfabrication of optical and photocatalytic elements.

Introduction

Since its discovery in 1995,^{1,2} the phenomenon of photo-induced mass migration in azobenzene (Az)-containing organic polymer films, leading to the surface relief formation, has attracted great attention from materials chemists and physicists. This phenomenon is dubbed as photoinduced surface relief gratings (SRG) or photoinduced relief formation (PRF).^{3–5} In this process, the trans–cis photoisomerization taking place at the molecule level is transformed to the dynamic transfer motions that reach to distances of more than micrometer levels. At the early stage of research, the systems are mostly limited to amorphous Az-containing polymer films;^{1–5} however, recent activities have been rapidly accumulating new knowledge, expanding to other types of materials including amorphous low-molecular-mass compounds^{6,7} and even the surface of molecular crystals.⁸ In view of chemical design of materials,

many new attempts have recently been made. SRG systems based on the supramolecular basis (noncovalent attachment of the Az unit in the polymer design) are demonstrated,^{9,10} and moreover, photochromic units other than Az, such as spiropyrans¹¹ and diarylethens,¹² have also been investigated.

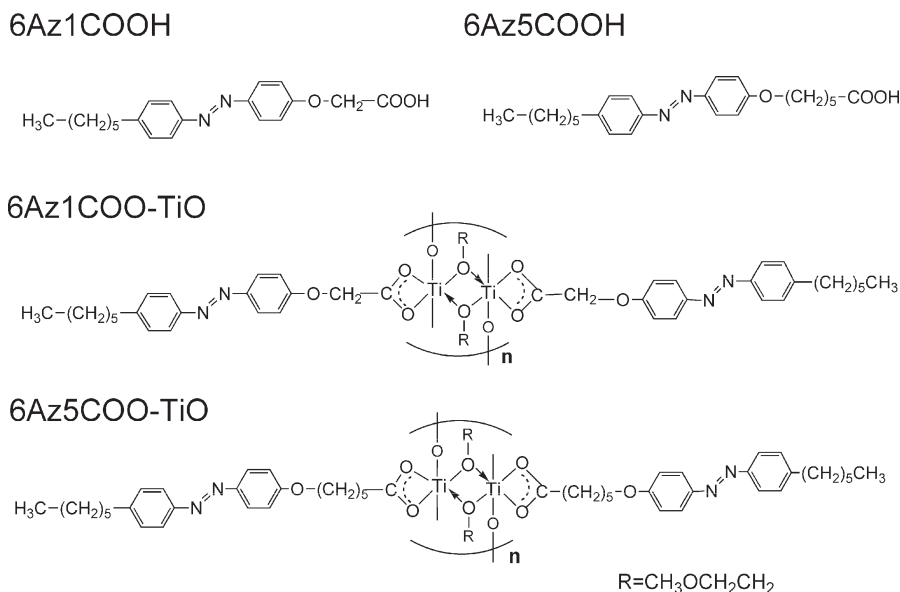
Our work has focused on liquid crystalline (LC) Az-polymer materials for SRG formation.^{13–16} The mass migration is completed at uncommonly small dose levels (< 100 mJ cm⁻²), which is 3 orders of magnitude smaller than those required for conventional amorphous polymer films.¹⁷ Here, the Az unit providing a long lifetime of cis-isomer is employed, and thus the photoirradiation with UV (365 nm) light leads to the smectic LC to isotropic phase transition.¹⁸ The mass transport in the LC polymers occurs at boundary areas between the smectic LC and isotropic phases.¹⁶ Besides the high sensitivity, the mass migration in the LC polymers has

*Corresponding author. E-mail: tseki@apchem.nagoya-u.ac.jp.

- (1) Rochon, P.; Batalla, E.; Natansohn, A. *Appl. Phys. Lett.* **1995**, *66*, 136.
- (2) Kim, D. Y.; Tripathy, S. K.; Li, L.; Kumar, J. *Appl. Phys. Lett.* **1995**, *66*, 1166.
- (3) Natansohn, A.; Rochon, P. *Chem. Rev.* **2002**, *102*, 4139.
- (4) Viswanathan, N. K.; Kim, D. Y.; Bian, S.; Williams, J.; Liu, W.; Li, L.; Samuelson, L.; Kumar, J.; Tripathy, S. K. *J. Mater. Chem.* **1999**, *9*, 1941.
- (5) Yager, K. J.; Barrett, C. J. *Curr. Opin. Solid State Mater. Sci.* **2001**, *5*, 487.
- (6) Nakano, H.; Takahashi, T.; Kadota, T.; Shiota, Y. *Adv. Mater.* **2002**, *14*, 1157.
- (7) Ishow, E.; Lebon, B.; He, Y.; Wang, X.; Bouteiller, L.; Galmeche, L.; Nakatani, K. *Chem. Mater.* **2006**, *18*, 1261.
- (8) Nakano, H.; Tanino, T.; Shiota, Y. *Appl. Phys. Lett.* **2005**, *87*, 061910/1–3.

- (9) Kulikovska, O.; Goldenberg, L. M.; Stumpe, J. *Chem. Mater.* **2007**, *19*, 3343.
- (10) Zettsu, N.; Ogasawara, T.; Mizoshita, N.; Nagano, S.; Seki, T. *Adv. Mater.* **2008**, *20*, 516.
- (11) Ubukata, T.; Takahashi, K.; Yokoyama, Y. *J. Phys. Org. Chem.* **2007**, *20*, 981.
- (12) Ubukata, T.; Yamaguchi, S.; Yokoyama, Y. *Chem. Lett.* **2007**, *36*, 1224.
- (13) Ubukata, T.; Seki, T.; Ichimura, K. *Adv. Mater.* **2000**, *12*, 1675.
- (14) Zettsu, N.; Ubukata, T.; Seki, T.; Ichimura, K. *Adv. Mater.* **2001**, *13*, 1693.
- (15) Zettsu, N.; Seki, T. *Macromolecules* **2004**, *37*, 8692.
- (16) Zettsu, N.; Ogasawara, T.; Arakawa, R.; Nagano, S.; Ubukata, T.; Seki, T. *Macromolecules* **2007**, *40*, 4607.
- (17) Seki, T. *Curr. Opin. Solid State Mater. Sci.* **2006**, *10*, 241.
- (18) Ikeda, T. *J. Mater. Chem.* **2003**, *13*, 2037.

Scheme 1. Chemical Structures of the Az Derivatives and Organic–Inorganic Hybrids



characteristic features such as (i) the process is insensitive to the light polarization,¹⁹ (ii) the motion continues even after stopping the irradiation,²⁰ and (iii) the motion is promoted by the sensitization from a dye absorbing longer wavelength.¹⁶ All these facts support the idea that the driving mechanism in the LC polymer systems is fully different from those studies for the amorphous ones. The migration occurs thermally via self-assembly of the film material, and the electromagnetic effect (gradient force) considered for the conventional-type,⁵ if any, is negligible.¹⁷

On the other hand, organic–inorganic nanohybrids synthesized via the sol–gel reaction containing organic components have been the subject of particular significance in material nanotechnologies, and an explosive number of investigations have been undertaken.^{21–23} The organic–inorganic hybrid materials have superior features possessing both flexibility and functionality of organic components and chemical, thermal, and mechanical stability of inorganic ones. Despite this large stream of research, however, little effort has been made to fabricate hybrid systems that show photoinduced mass migration. In this respect, Darracq et al.²⁴ reported a pioneering work using Az-containing silica-based sol–gel system. They succeeded in fabricating the SRGs on the hybrid film by irradiation with interference Ar⁺ laser beam, but in this amorphous type hybrid a vast amount of recording energy as 60–140 J cm⁻² (0.6–1.4 J mm⁻² in the paper) is required.²⁴ More recently, Kulikovska et al.²⁵ reported a supramolecular sol–gel

material system based on the ionic interaction between an oppositely charged Az unit and silica for optical generation of surface relief structures. The modulation depths of the recorded gratings were large, but also in this type hybrid material, a vast amount of recording energy as 30–900 J cm⁻² was required. Hybrid systems that work at moderate energy doses are highly desired.

The above knowledge in mind, we propose herein a newly designed “liquid crystalline” organic–inorganic material that exhibits an efficient phototriggered mass transport behavior. This manuscript describes the synthesis, characterizations and preliminary results on the phototriggered motions. The inorganic component used in this study is titanium oxide, which is anticipated to be converted to photofunctional materials such as photocatalyst via a suitable pyrolytic process after inscription of any desired relief structure is made. A new platform based on the organic–inorganic hybridization is proposed in the photoinscription of surface reliefs.

Experimental Section

Synthesis. Organic–inorganic hybrid materials used in this study were synthesized using an Az derivative (6Az5COOH or 6Az1COOH, Scheme 1) and titanium tetra-isopropoxide (Ti(O-*i*-Pr)₄). The prepared hybrid materials are abbreviated as 6Az5COO-TiO or 6Az1COO-TiO. The synthesis of 6Az5COOH and 6Az1COOH was reported in the previous paper.²⁶ The hybrid materials, 6Az5COO-TiO and 6Az1COO-TiO, were prepared by mixing the corresponding Az carboxylic acid with Ti(O-*i*-Pr)₄ in 2-methoxyethanol.²⁷ The molar ratio of 6Az5COOH or 6Az1COOH and Ti(O-*i*-Pr)₄ was adjusted to be 1:1. The solution was stirred at room temperature until both reagents were dissolved completely (typically at 15 °C for about 30 min). The proceeding of the coordination between titanium and Az carboxylate was monitored by Fourier transform infrared (FT-IR) spectroscopy.

- (19) Zetsu, N.; Fukuda, T.; Matsuda, H.; Seki, T. *Appl. Phys. Lett.* **2003**, *83*, 4960.
 (20) Ubukata, T.; Hara, M.; Ichimura, K.; Seki, T. *Adv. Mater.* **2004**, *16*, 220.
 (21) Luand, G. Q.; Zhao X. S.; eds. *Nanoporous Materials—Science and Engineering*; Imperial College Press: London, 2004.
 (22) Hoffmann, F.; Cornelius, M.; Morell, J.; Froba, M. *Angew. Chem., Int. Ed.* **2006**, *45*, 3216.
 (23) Fujita, S.; Inagaki, S. *Chem. Mater.* **2008**, *20*, 891.
 (24) Darracq, B.; Chaput, F.; Lahli, K.; Levy, Y.; Boilot, J. P. *Adv. Mater.* **1998**, *10*, 1133.
 (25) Kulikovska, O.; Goldenberg, L. M.; Kulikovskiy, L.; Stumpe, J. *Chem. Mater.* **2008**, *20*, 3528.

- (26) Seki, T.; Sakuragi, M.; Kawanishi, Y.; Suzuki, Y.; Tamaki, T.; Fukuda, R.; Ichimura, K. *Langmuir* **1993**, *9*, 211.
 (27) Nishizawa, K.; Miki, T.; Fukaya, H.; Masuda, Y.; Suzuki, K.; Kato, K. *Thin Solid Films* **2008**, *516*, 2635.

After 6Az5COOH or 6Az1COOH and $\text{Ti}(\text{O-}i\text{-Pr})_4$ were fully coordinated, the solution was dried at room temperature in a vacuum oven to yield a powder sample.

Measurements. FT-IR measurements were performed using an FTS 7000HS (Bio-Rad laboratory, Inc.). For the obtained hybrids, FT-IR spectroscopy measurements were performed by the KBr method. ^1H NMR spectra of the hybrids were recorded on a JNM-A400 spectrometer (JEOL Co. Ltd.). Mass spectrometry of the hybrids was carried out by the matrix assisted laser desorption ionization-time-of-flight mass spectrometry (MALDI-TOF mass). MALDI-TOF mass measurements were performed using an Autoflex instrument (Bruker Daltonics, Inc.) using α -cyano-4-hydroxy cinnamic acid as a matrix. The hybrid was dispersed in a matrix/chloroform solution and deposited onto a stainless steel target plate. Desorption and ionization of the hybrid were achieved by irradiation of N_2 laser (wavelength: 337 nm). Elemental analysis of C, H, and N was carried out in an elemental analyzer Thermo Finnigan Flash EA 1112. The contents of O and Ti were determined by subtracting the amounts of C, H, and N from the total. Differential scanning calorimetry (DSC) profiles were taken on a DSC120U (Seiko Instruments, Inc.) with a scanning rate of $2\text{ }^\circ\text{C min}^{-1}$ on both heating and cooling processes. Polarized optical microscope (POM) observations were performed with a BH-2/DP70 system (Olympus Co. Ltd.) equipped with a Mettler FP82HT hot stage. UV-visible absorption spectra were taken on a U-4100 (HITACHI, Co. Ltd.). X-ray diffraction (XRD) measurements were made with an FR-E instrument and NANO viewer system (Rigaku Co. Ltd.) using an imaging plate. The surface topography of the films was observed using an atomic force microscopy (AFM, Nanopics 2100, Seiko Instruments, Inc.). Thickness of the films was also estimated by AFM after scratching the films with a spatula.

Methods. A powder of the hybrid, 6Az5COO-TiO or 6Az1COO-TiO, was dissolved in chloroform (1 wt %), and was spin-coated on a fused silica plate at 2000 rpm for 30 s. The synthesized hybrid materials were sensitive to ambient humidity. Therefore, the film was subjected to the irradiation immediately (typically within 30 s) for the relief formation. UV light (365 nm, nonpolarized) irradiation was performed using a Hg-Xe lamp (Supercure-203S, San-ei Electric, Co. Ltd.) passing through a combination of optical filters (UV-35 and UV-D35, Toshiba Co. Ltd.). A 10 μm line-and-space patterned photomask was used for the mass transport. Irradiation was made on a temperature controlled plate using a digital hot plate (PMC-720, Iuchi Seisakusho Co. Ltd.).

Results and Discussion

Structural Characterizations. The chemical structure of organic-inorganic hybrid materials synthesized in this study was characterized as follows.

In the FT-IR spectrum of 6Az5COOH, an intense peak at 1700 cm^{-1} , originating from the carboxyl group of 6Az5COOH was observed as shown in Figure 1a. In contrast, upon hybridization with $\text{Ti}(\text{O-}i\text{-Pr})_4$, this peak completely disappeared and new two peaks at 1534 and 1454 cm^{-1} , appeared (Figure 1b). These peaks were assignable to the antisymmetric and symmetric stretching vibration bands of carboxylate, respectively. These results indicate that the titanium metal of $\text{Ti}(\text{O-}i\text{-Pr})_4$ is coordinated with the carboxyl group of the Az compound. When $\text{Ti}(\text{O-}i\text{-Pr})_4$ was simply dissolved in 2-methoxyethanol followed by drying (abbreviated as TiO), a clear broadband around 3300 cm^{-1} originating

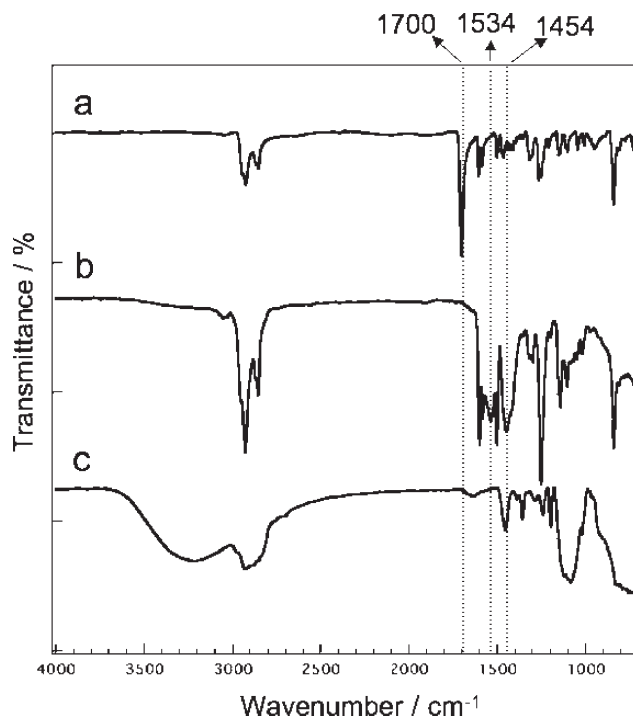


Figure 1. FT-IR spectra of (a) 6Az5COOH, (b) 6Az5COO-TiO hybrid material, and (c) TiO. TiO was prepared from $\text{Ti}(\text{O-}i\text{-Pr})_4$ dissolved in 2-methoxyethanol followed by drying without adding 6Az5COOH.

from the O-H stretching of hydroxy groups was observed (Figure 1c). However, for the hybrid system, the peak assignable to the hydroxy groups was hardly observed (Figure 1b). Therefore, the formation mechanism and the resulting structure of the Ti-O-Ti inorganic networks in the hybrid seem to differ from that in the TiO.

In the ^1H NMR spectrum of the 6Az5COO-TiO hybrid material (Supporting Information), no signal of carboxylic acid of 6Az5COOH was admitted, showing that the hybridization is fully achieved. In addition, the signals originating from isopropoxide group of $\text{Ti}(\text{O-}i\text{-Pr})_4$ were not observed, and instead three peaks assignable to 2-methoxyethoxy groups were observed in the range from 3.74 to 3.40 ppm. Thus, the isopropoxide group of $\text{Ti}(\text{O-}i\text{-Pr})_4$ was fully exchanged with 2-methoxyethanol.

In the MALDI-TOF mass spectrum, the parent peak (M^+) of the 6Az5COO-TiO hybrid was obtained at 1068. This mass value corresponds to the “dimerized” hybrid structure of 6Az5COO-TiO. The same results were obtained also for 6Az1COO-TiO. The most probable chemical structures of these hybrids based on these analytical data and the previous knowledge^{27,28} are indicated in Scheme 1. Bradley, et al. reported that titanium tetraethoxides in a dilute alcoholic solution are not effectively polymerized but consist of dimeric species of $\text{Ti}_2(\text{OEt})_8 \cdot (\text{EtOH})_2$, due to the solvation.²⁹ Our results are in agreement with their observation.

The CHN elemental analysis of the 6Az5COO-TiO hybrid further justified the dimer formation. The found values of elemental analysis (C, 59.54; H, 6.96; N, 5.61; O + Ti, 27.89) closely agreed with those of the calculated ones (C, 60.67;

(28) Doeuff, S.; Henry, M.; Sanchez, C.; Livage, J. J. *Non-Cryst. Solids* **1987**, *89*, 206.

(29) Bradley, D. C. *Coord. Chem. Rev.* **1967**, *2*, 299.

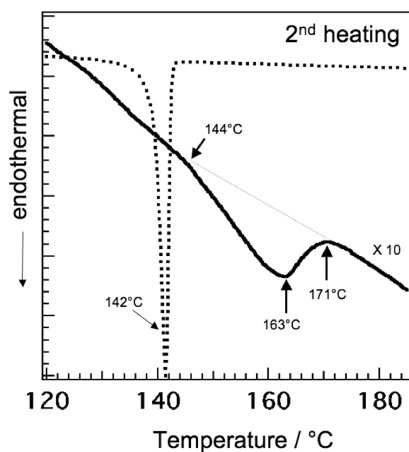


Figure 2. DSC curves of 6Az5COOH (dotted line) and 6Az5COO-TiO (solid line) on the second heating process. Heating rate is $2\text{ }^{\circ}\text{C min}^{-1}$.

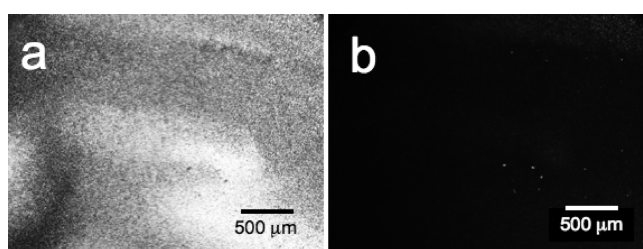


Figure 3. POM images of 6Az5COO-TiO at (a) room temperature and at (b) $145\text{ }^{\circ}\text{C}$, respectively (magnification: $\times 30$).

H, 7.12; N, 5.24; O + Ti, 26.97) for $\text{C}_{54}\text{H}_{76}\text{N}_4\text{O}_{12}\text{Ti}_2$ based on the dimer structure shown in Scheme 1.

Liquid Crystalline Properties of Hybrid Material. The DSC measurements and POM observations were performed for the hybrids. Figure 2 shows the DSC curves of 6Az5COOH (dotted line) and 6Az5COO-TiO (solid line) on the second heating. 6Az5COOH gave a sharp endothermic peak at $142\text{ }^{\circ}\text{C}$ on heating (transition enthalpy, 88.0 mJ mg^{-1}), corresponding to the melting of this compound. In contrast, 6Az5COO-TiO showed no peak around this temperature, and instead a broad endothermic peak was observed in the range from 144 to $171\text{ }^{\circ}\text{C}$. Also, the transition enthalpy became significantly small (4.9 mJ mg^{-1}). Thus, the thermal properties of 6Az5COO-TiO was essentially different from that of 6Az5COOH, indicating the full complexation of the two components without retention of the pure 6Az5COOH derivative. The POM image of 6Az5COO-TiO at room temperature showed a sandlike texture (Figure 3a), which is frequently observed for side-chain type polymers that shows a smectic phase, suggesting that this organic-inorganic hybrid adopts the smectic phase. The sandlike texture of 6Az5COO-TiO was clearly observed up to $140\text{ }^{\circ}\text{C}$, and it changed dramatically to a dark image reflecting the thermally induced isotropic phase above $145\text{ }^{\circ}\text{C}$ (Figure 3b). Upon UV irradiation at $125\text{ }^{\circ}\text{C}$, the sandlike texture rapidly changed to a dark image indicating the procedure of the photochemically induced smectic to isotropic phase transition.

In contrast, 6Az1COO-TiO without a flexible methylene spacer showed no appreciable DSC peaks in these

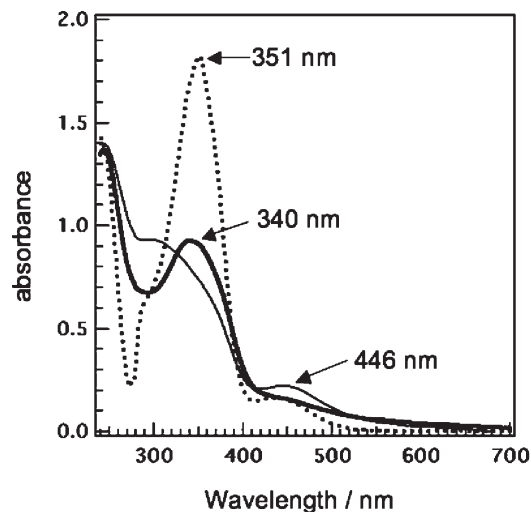


Figure 4. UV-visible absorption spectra of 6Az5COO-TiO dissolved in chloroform (dotted line) and a spincast film on a fused silica plate before (thick solid line) and after (thin solid line) UV irradiation.

regions, suggesting that this hybrid does not show the liquid crystallinity. Therefore, the present study hereafter focuses onto the 6Az5COO-TiO hybrid.

Figure 4 shows UV-visible absorption spectra of 6Az5COO-TiO in chloroform (dotted line), in the film state before (solid wide line) and after (solid thin line) UV light irradiation on a fused silica plate. The absorption maximum (λ_{max}) of the π - π^* long-axis transition of Az in chloroform was positioned at 351 nm , whereas that of the spincast film was located at 340 nm . This fact indicates that the Az units partially form H-type aggregates in the spincast film.¹⁵ The molecular orientation of the azobenzene units can be roughly estimated by the ratio of absorption intensities at the π - π^* long-axis transition of Az (around 350 nm) to the π - π^* transition of phenyl (244 nm , often expressed as ϕ - ϕ^*) bands, because the direction of the π - π^* long-axis transition of Az is directionally dependent while that of the π - π^* transition of phenyl is essentially insensitive to the Az orientation.³⁰ The ratios of $A_{\pi-\pi^*(\text{Az})}/A_{\pi-\pi^*(\text{phenyl})}$ in the chloroform solution and for the spincast film were 1.33 and 0.68, respectively. These spectral data indicate that the Az units preferentially adopt a perpendicular orientation to the substrate in the films. This perpendicular orientation of mesogenic groups are commonly observed for organic side-chain LC polymer films.^{31,32} As shown for the spectrum of thin solid line, the spectrum of the spincast film changed after UV irradiation. The absorbance of the long-axis π - π^* transition of Az in the trans form (340 nm) decreased, and instead that of the n - π^* transition (around 450 nm) increased. It is thus obvious that the trans-to-cis photoisomerization of Az undergoes in the hybrid film by irradiation with UV light. The thermal cis-to-trans back reaction proceeded in a range of hours as usually observed for this Az derivative (see the Supporting Information).

(30) Uekusa, T.; Nagano, S.; Seki, T. *Langmuir* **2007**, *23*, 4642.

(31) Geue, T.; Ziegler, A.; Stumpe, J. *Macromolecules* **1997**, *30*, 5729.

(32) Han, M.; Morino, S.; Ichimura, K. *Chem. Lett.* **1999**, 645.

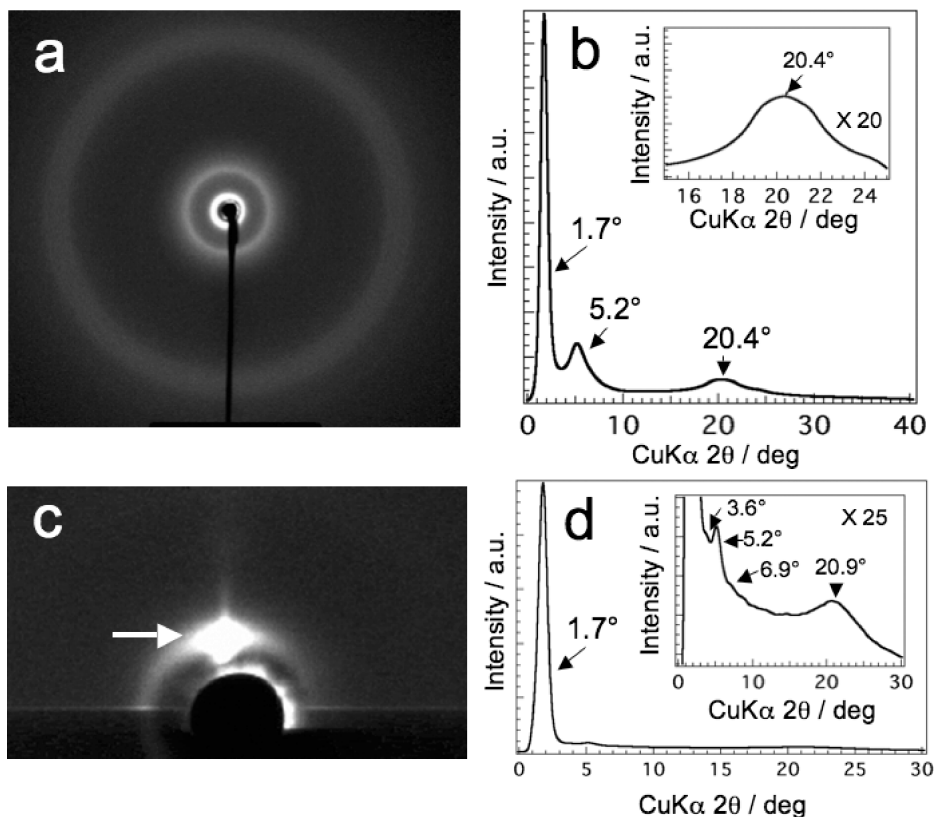


Figure 5. (a) 2D XRD pattern of 6Az5COO-TiO hybrid measured by the capillary method at room temperature, (b) 1D profile extracted from the 2D XRD pattern of a, (c) 2D GI-XRD pattern of the spincast 6Az5COO-TiO film recorded on an imaging plate, and (d) 1D profile in the out-of-plane direction extracted from the 2D XRD pattern of c. In c, the first diffraction spot in the out-of-plane direction is indicated as a bold arrow.

Figure 5a and 5b show XRD data of 6Az5COO-TiO measured by the capillary method in 2D image taken on an imaging plate (a) and an extracted 1D profile (b) at room temperature. A clear peak was observed at $2\theta = 1.7^\circ$, which corresponds to a (100) layer spacing (d) of 5.2 nm. This spacing almost corresponds to a double length of the organic Az component. In addition, the (300) diffraction peak was also observed at $2\theta = 5.2^\circ$ ($d = 1.7$ nm). A broad diffraction band was observed at $2\theta = 20.4^\circ$ ($d = 0.43$ nm) in the wider angle region, corresponding to the packing of Az units. These data strongly suggest that 6Az5COO-TiO adopt a smectic LC phase (probably, smectic A) at room temperature.

The molecular orientation of 6Az5COO-TiO in the spincast film on the substrate was investigated by the grazing angle (GI)-XRD measurement (Figures 5c and 5d). As shown in Figure 5c, an intense diffraction spot was observed in the out-of-plane direction, which is derived from the smectic layer oriented parallel to the substrate. The extracted 1D profile indicates that a clear peak was observed at $2\theta = 1.7^\circ$ (Figure 5d), in agreement with that for the capillary method. For the film, the periodic diffraction peaks to the fourth orders were observed in the out-of-plane direction as shown in the inset [$2\theta = 1.7^\circ$ ($d = 5.2$ nm), 3.6° (2.5 nm), 5.2° (1.7 nm), and 6.9° (1.3 nm)]. On the other hand, only weak diffraction spots were observed in the in-plane direction (Figure 5c). In this way, the highly oriented smectic layer orienting parallel to the substrate was obtained by spincasting.

Together with the data of XRD and UV-visible spectroscopic measurements, one can draw a schematic illustration

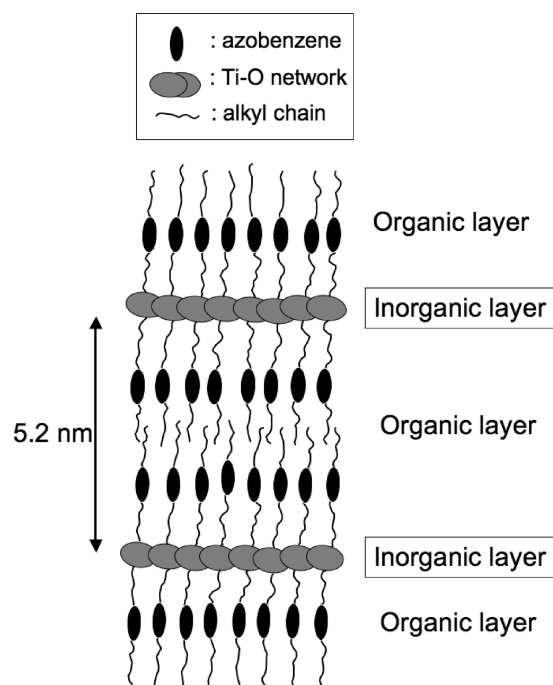


Figure 6. Schematic illustration of the plausible molecular structure of the spincast film of 6Az5COO-TiO hybrid.

for the molecular structure for the spincast film of 6Az5COO-TiO hybrid as shown in Figure 6. The organic 6Az5COO- and inorganic TiO components are oriented perpendicular and parallel to the substrate, respectively, to form a smectic LC layer structure. This structure closely resembles the layer structure observed for the films of

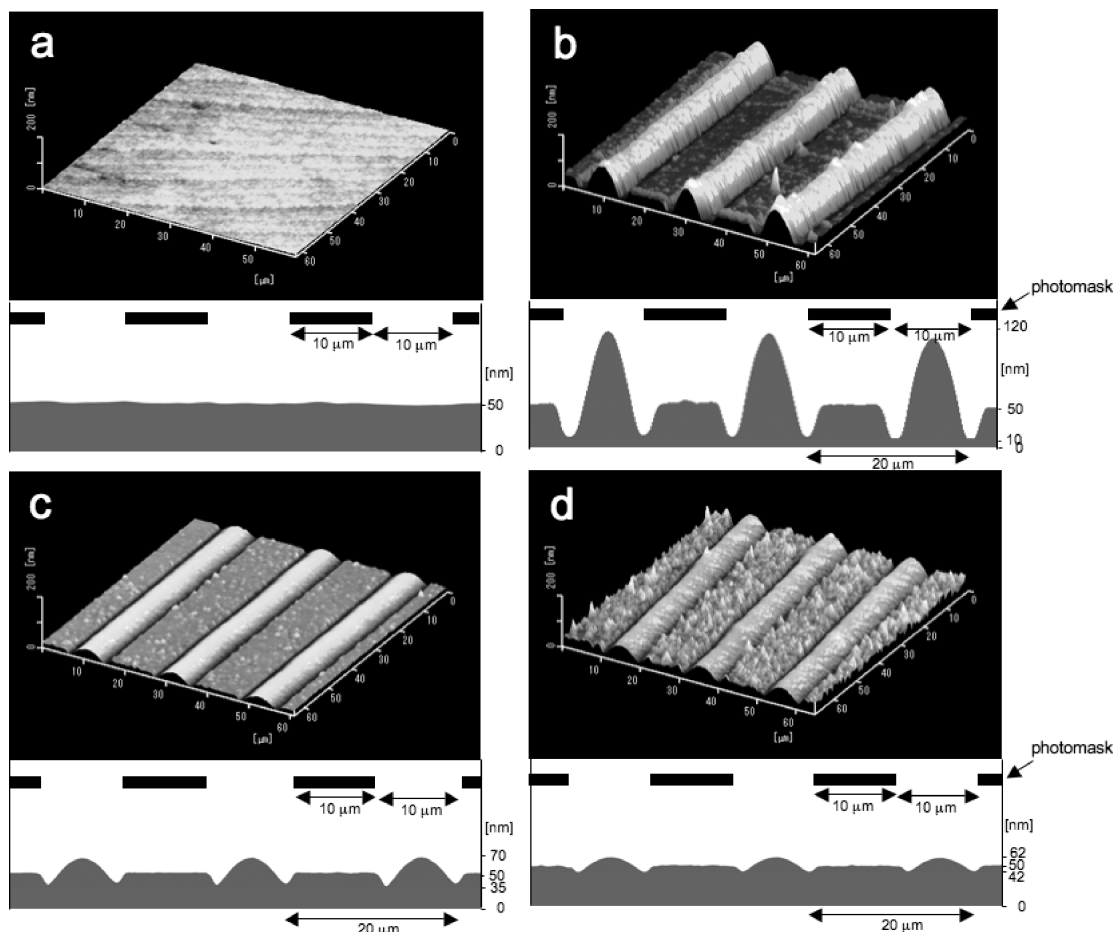


Figure 7. Topographical AFM images and cross-sectional height profiles of the 6Az5COO-TiO hybrid film after exposure of UV (365 nm, 8 mW cm^{-1}) for 500 s) light through a $10 \mu\text{m}$ line-and-space photomask at various temperatures, (a) room temperature ($15 \text{ }^\circ\text{C}$), (b) $125 \text{ }^\circ\text{C}$, (c) $135 \text{ }^\circ\text{C}$, and (d) $145 \text{ }^\circ\text{C}$. The full Z range for all surface images is 200 nm.

smectic LC polymer of side-chain type. Organic–inorganic self-assembled hybrid materials forming columnar structures are already known,^{33,34} and for layer-forming systems, the sol–gel process has been applied in the presence of side-chain LC polymers.^{35,36} However, to the best of our knowledge, this is the first example of the self-assembled LC hybrid system that is formed from the nanophase separation between the inorganic part (TiO) and the organic one (6Az5COO–).

Photo-Triggered Surface Relief Formation. Since the smectic LC hybrid system was successfully synthesized, the film has subsequently been subjected to the photoinduced

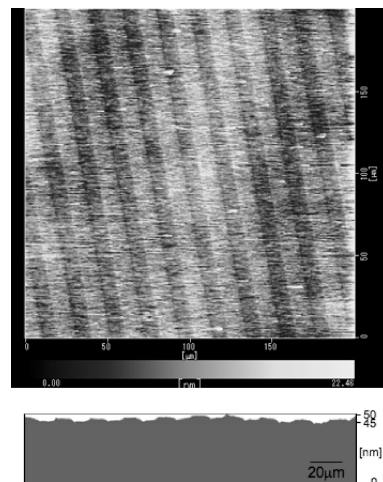


Figure 8. Topographical AFM image of the 6Az5COO-TiO hybrid film exposed with UV (365 nm , 8 mW cm^{-1}) light through a $10 \mu\text{m}$ line-and-space photomask for 5 s at $125 \text{ }^\circ\text{C}$ after keeping at the same temperature for 1 min before UV exposure.

- (33) Cho, B.-K.; Jain, A.; Mahajan, S.; Ow, H.; Gruner, S. M.; Wiesner, U. *J. Am. Chem. Soc.* **2004**, *126*, 4070.
- (34) Kimura, M.; Wada, K.; Ohta, K.; Hanabusa, K.; Shirai, H.; Kobayashi, N. *J. Am. Chem. Soc.* **2001**, *123*, 2438.
- (35) Perreora, F. V.; Merlo, A. A.; Bley, F.; Morfin, I.; Ritter, O. M.; da Silveira, N. P.; Ehrburger-Dolle, F. *Liq. Cryst.* **2008**, *35*, 299.
- (36) da Silveira, N. P.; Ehrburger-Dolle, F.; Rigacci, A.; Perreora, F. V.; Westfahl, H. Jr. *J. Therm. Anal. Calorim.* **2005**, *79*, 579.
- (37) In our original procedure for the surface relief inscription on the LC polymer films, patterned irradiation with blue visible light (488 nm argon ion laser beam or 436 nm line from a Hg lamp) have been performed after preillumination with a 365 nm line from a Hg lamp over the polymer film area.^{13,14} Our recent investigations have revealed that the mass transfer also occurs via a simple one-step irradiation with 365 nm light through a photomask, provided that the *trans*-Az film is in the smectic LC state at controlled temperatures. This work adopts this patterned UV irradiation method.

inscription. Figure 7 shows the topographical AFM images of the hybrid film after exposure to UV light (365 nm)³⁷ at an energy dose of 4 J cm^{-2} (8 mW cm^{-2} for 500 s) through a $10 \mu\text{m}$ line-and-space photomask at various temperatures. The initial film was flat with ca. 50 nm thickness. The efficiency of surface relief formation showed a clear

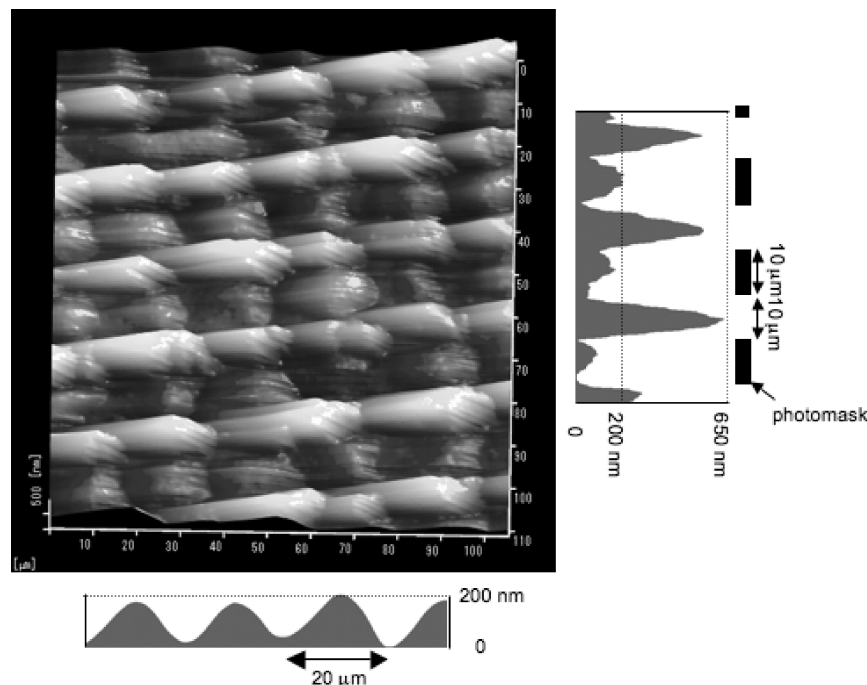


Figure 9. Topographical AFM image of the doubly inscribed 6Az5COO-TiO hybrid film exposed to UV (365 nm, 8 mW cm^{-2} for 500 s) light through a $10 \mu\text{m}$ line-and-space photomask for 500 s at $125 \text{ }^\circ\text{C}$. The first inscription was achieved in the vertical direction, followed by the second inscription in the horizontal direction.

temperature dependency. The relief formation was not observed at room temperature (Figure 7a) and irradiation at $115 \text{ }^\circ\text{C}$ gave only a small relief inscription (data not shown). On the other hand, the relief structure was obviously generated at $125 \text{ }^\circ\text{C}$ as shown in Figure 7b. The height difference from the peak to valley was ca. 110 nm, and the thickness in the lowest areas from the substrate surface was ca. 10 nm. In the cross-section profiles, the protruded area almost corresponded to the total of two depressed ones. Thus, the corrugation features clearly indicate that the relief formation is caused by the mass transfer. The material migration occurred at the boundary from the nonilluminated regions to UV-irradiated ones.³⁸ The resulting relief structure was not a simple undulation, but consisted of regularly arrayed protrusions with depressions in both sides and flat regions. Such features are characteristics after irradiation through a line-and-space photomask with larger widths.³⁹ With regard to the concentration of the chloroform solution for the spincoat, 1 wt % was found to be optimum to exert the efficient surface relief formation. When the film was fully dried and the condensation reaction proceeded to some extents in hybrid film, the mass transport was impeded. Thus, the photoirradiation was achieved within 30 s after the spin-coating as described in the experimental section.

At a moderately higher temperature ($135 \text{ }^\circ\text{C}$), essentially the same relief was obtained but the top-to-valley

height difference was reduced to 30–40 nm (Figure 7c). The unirradiated surface area became rough at $145 \text{ }^\circ\text{C}$ (Figure 7d), and the corrugation formation was hardly recognized at a further elevated temperature of $160 \text{ }^\circ\text{C}$ (data not shown). In this way, the optimal temperature range was around $130 \text{ }^\circ\text{C}$, which corresponds to the lower edge of the endothermic peak in the DSC profile (Figure 2). It is likely that at temperatures below the thermal phase transition, the viscosity is too high to induce mass transfer at micrometer distances. On the other hand, at the melting temperature (ca. $160 \text{ }^\circ\text{C}$), the smectic LC characteristics required for the collective motional cooperativity is lost, leading to the lack of mass transfer motions.

In a separate experiment, the energy dose of 0.8 J cm^{-2} (8 mW cm^{-2} for 100 s) at $125 \text{ }^\circ\text{C}$, was found to be sufficient for the photoinscription, which is ca. 100–1000 times less than that reported by Darracq et al. ($60\text{--}140 \text{ J cm}^{-2}$)²⁴ and Kulikovska et al. ($30\text{--}900 \text{ J cm}^{-2}$).²⁵ To our surprise, the relief structure was already initiated at a very small dose of 0.04 J cm^{-2} (8 mW cm^{-2} for 5 s) at $125 \text{ }^\circ\text{C}$ as shown in Figure 8. This light dose is comparable to the level of fully organic soft LC polymer systems.^{13–17} These facts strongly suggest that the mass migration is brought about via cooperative and collective motions. In the case of the nonliquid crystalline system of 6Az1COO-TiO, the mass transfer was not observed at any temperature. This fact further supports the importance of liquid crystallinity for the efficient mass transfer process.

The obtained relief structure was mechanically stable and remained unchanged for at least a month at room temperature. Also, the inscribed relief structure was not erased after heating at $250 \text{ }^\circ\text{C}$ or UV irradiation at $125 \text{ }^\circ\text{C}$. Only slight deformation was observed after such

(38) Our former investigation showed that when patterned irradiation with 436 nm light is performed after preirradiation with 365 nm light, the mass migration occurs from the illuminated areas to unilluminated ones (see refs 13, 14, and 20). The migration direction in this study is seemingly opposite, i.e., the material migrates toward the illuminated areas. However, both processes have common features in that the migration occurs from the areas in the smectic LC state to those in the isotropic one.

(39) Ubukata, T.; Higuchi, T.; Zetsu, N.; Seki, T.; Hara, M. *Colloids Surf., A* **2005**, 257–258, 123.

procedures, which was not correlated with the thermal back isomerization of the Az unit (see Figure S3 in the Supporting Information). Most probably, the network formation of the titanium oxide layer resists to morphology relaxations. However, if appropriate conditions were provided retaining some fluidity in the film, a stepwise inscription was found to be attained. Figure 9 shows an example of the relief structure inscribed by a two-step orthogonal irradiation at 125 °C. UV irradiation through a photomask was first performed on the film for 500 s in the same conditions as Figure 7b. The film was maintained at 125 °C for 500 s throughout the two-step irradiation. The interval between the first and the second irradiation was 500 s. The second inscription was subsequently performed on the same area by rotating the sample by 90°. As the consequence, a complicated 2D patterned figure was inscribed on the film. Interestingly, the final height reached over 600 nm after the two step inscription. We noticed that the height was further enhanced only by heating at 125 °C for 500 s. Therefore, the relief formation seems to involve both the photo-triggered transfer and a thermally induced reaction/diffusion process (embossing effect).⁴⁰

Conclusion

A novel organic–inorganic LC hybrid material, 6Az5-COO-TiO, was synthesized. This hybrid shows a smectic LC (probably smectic A) and isotropic phases in the trans

and cis forms of Az, respectively. This can be a new class of LC hybrid material formed via the nanophase separation of the organic and inorganic components. The mass transfer was performed by patterned UV irradiation of very low energy doses (ca. 100 – 1000 times less than hitherto known sol–gel materials) at temperatures around 130 °C. Because no transfer occurred for the non-LC analogue of 6Az1COO-TiO hybrid, the importance of the cooperative nature of liquid crystallinity is suggested for the driving force of the relief formation. The detailed analyses of the mass transfer mechanism and investigations for the optimization of the process are now in progress. Toward applications, one of the alluring strategies is to remove organic components to provide titania films retaining the designed relief morphologies. Effort in this direction is also underway. It is stressed that because of the facile and versatile synthetic procedure, the set of organic and inorganic components is not limited, but large variations of material combination are anticipated.

Acknowledgment. We thank Shun Mitsui and Seiichiro Kodama of Nagoya University for their helpful technical assistance. This work was supported by a Grant-In-Aid Scientific Research for Priority Areas “New Frontiers in Photochromism (no. 471)” of MEXT, Japan.

Supporting Information Available: Analytical data of ¹H NMR, mass spectrum of the 6Az5COO-TiO hybrid material, and UV–visible absorption spectra showing the proceeding of thermal cis-to-trans isomerization (PDF). This material is available free of charge via the Internet at <http://pubs.acs.org>.

(40) Sánchez, C.; de Gans, B.-J.; Kozodaev, D.; Alexeev, A.; Escuti, M. J.; van Heesch, C.; Bel, T.; Schubert, U. S.; Bastiaansen, C. W. M.; Broer, D. J. *Adv. Mater.*, 2005, 17, 2567.